Analytic Equation of State and Thermodynamic Properties for α-, β-, and γ-Si_3N_4 Based on Analytic Mean Field Approach

L.G. Wang, J.X. Sun*, W. Yang and R.G. Tian

Department of Applied Physics, University of Electronic Science and Technology
Chengdu 610054, P.R. China

(Received January 7, 2008; revised version April 15, 2008; in final form May 19, 2008)

The analytic mean field potential approach is applied to α-, β-, and γ-Si_3N_4. The analytic expressions for the Helmholtz free energy, internal energy, and equation of state were derived. The formalism for the case of the Morse potential is used in this work. Its six potential parameters are determined through fitting the compression experimental data of α-, β-, and γ-Si_3N_4. The calculated compression curves of α-, β-, and γ-Si_3N_4 are in good agreement with the available experimental data. This suggests that the analytic mean field potential approach is a very useful approach to study the thermodynamic properties of Si_3N_4. Furthermore, we predict the variation of the free energy and internal energy with the molar volume at several higher temperatures and calculate the temperature dependence of the molar volume, bulk modulus, thermal expansion coefficient and isochoric heat capacity at zero pressure.

PACS numbers: 64.10.+h, 65.40.−b, 61.66.Fn

1. Introduction

Silicon nitride (Si_3N_4) is currently one of the most important technical materials owing to its unique mechanical and electronic properties. It is well known that there are two stable polymorphs of silicon nitride, α- and β-Si_3N_4, where the β configuration is the more stable of the two [1]. Both have a hexagonal lattice and only differ along the z axis in the stacking sequence. It is generally believed that

*corresponding author; e-mail: sjx@uestc.edu.cn

α- and β-Si_3N_4 are low- and high-temperature polymorphs, respectively, with a transformation of α to β phase occurring at elevated temperatures above 1300°C. In 1999, a third polymorph of silicon nitride (γ-Si_3N_4) synthesized by Zerr et al. [2] under high-pressure and high-temperature conditions. It has a hardness comparable to the hardest known oxide (stishovite, a high-pressure phase of SiO_2) [2–6] and significantly greater than the hardness of α- and β-Si_3N_4 [7]. In recent years, many experiments on the properties of Si_3N_4 have been performed, and their theories have been studied [8–18]. Among all the properties of Si_3N_4 studied so far, the thermodynamic properties have been an intriguing subject. For example, Kruger et al. have measured the isothermal equation of state of α-Si_3N_4 by means of high-pressure X-ray diffraction, determining the bulk modulus and the linear incompressibilities [8]. Jiang et al. have reported the compressibility and thermal-expansion behavior of γ-Si_3N_4 by *in situ* X-ray powder-diffraction measurements using synchrotron radiation, complemented with computer simulations by means of first-principles calculations [9]. Paszkowicz et al. have determined the lattice parameter and thermal expansion coefficient of γ-Si_3N_4 under high-pressure and high-temperature conditions by X-ray diffraction [10]. Although there exist many reports on the thermodynamic properties of Si_3N_4, most of them are the experimental works.

However, we believe that the theoretical study on the thermodynamic properties of α-, β-, and γ-Si_3N_4 is very important for applications. Several years ago, Wang et al. [19–22] proposed the analytic mean field potential (AMFP) approach, and applied it to many materials. Bhatt et al. [23, 24] further applied the AMFP to lead and alkali metals, and concluded that in comparison with other theoretical models the AMFP is computationally simple, physically transparent and reliable to study the thermodynamic properties in the high pressures and high temperatures environment. Recently, Sun et al. have proven that the AMFP is an analytic approximation of the free volume theory (FVT) [25]. The FVT is a mean field approximation to the thermal contribution of atoms to the Helmholtz free energy of crystalline phases. It is more valuable to directly use the strict FVT than the approximate AMFP, in the cases that the analytic equation of state can be derived based on the strict FVT. Nevertheless, in some cases the mean-field integral and the equation of state (EOS) for the strict FVT are fairly complicated or cannot be analytically derived. Then it is convenient to develop simple analytic EOS through the AMFP, when the complete FVT fails. The AMFP has been applied to solid C_{60} by using the Girifalco potential [26] by Sun [27]; the numerical results are in good agreement with the molecular dynamics (MD) simulations [28, 29] and superior to the correlative method of unsymmetrized self-consistent field (CUSF) of Zubov et al. [30, 31]. This verifies that the AMFP is a convenient approach to consider the anharmonic effects at high temperature. Thus, in this paper, we present the results of thermodynamic properties of α-, β-, and γ-Si_3N_4 by using the AMFP.

The rest of this paper is organized as follows. In Sect. 2 we derive the analytic EOS based on the AMFP approach. In Sect. 3, the parameters of the Morse potential are determined by fitting the compression experimental data of α-, β-, and γ-Si_3N_4 and the numerical results of thermodynamic properties are calculated and compared with the experimental data. In Sect. 4 the conclusion is presented.

2. Analytic equation of state

In terms of the FVT, the free energy can be expressed as [32–38]:

$$\frac{F}{NkT} = -\frac{3}{2}\ln(2\pi\mu kT/h^2) + \frac{1}{kT}[E_1(a) + E_2(a)] - \ln\nu_{\rm f} + \frac{F_{\rm qm}}{NkT}, \tag{1}$$

where μ is the average mass per atom in Si_3N_4, $\nu_{\rm f}$ is the free volume,

$$\nu_{\rm f} = 4\pi\int_0^{r_{\rm m}} \exp(-g(r,V)/kT)r^2{\rm d}r. \tag{2}$$

$F_{\rm qm}/NkT$ is the quantum modification, by using the Einstein model, we have

$$\frac{F_{\rm qm}}{NkT} = \frac{F_{\rm q}}{NkT} - \lim_{T\to\infty}\left(\frac{F_{\rm q}}{NkT}\right) = 3\ln(1-{\rm e}^{-\Theta_{\rm E}/T}) - 3\ln(\Theta_{\rm E}/T). \tag{3}$$

$E_{\rm c}(a) = E_1(a) + E_2(a)$ is the cohesive energy of an atom, a is the nearest-neighbor distance. Based on the embedded atom model, $E_{\rm c}(a)$ can be divided into two parts: $E_1(a)$ and $E_2(a)$. For metal, the first part $E_1(a)$ represents the contribution of electron gas. As for Si_3N_4, we think that the first part $E_1(a)$ is the partial contribution of chemical bond. The second part $E_2(a)$ represents the contribution of the van der Waals interaction between atoms. By using the Morse potential, we have

$$\begin{cases} E_1(a) \equiv E_1(y_1) = \varepsilon_1[\exp(2\lambda_1(1-y_1)) - 2\exp(\lambda_1(1-y_1))], \\ E_2(a) \equiv E_2(y_2) = \varepsilon_2[\exp(2\lambda_2(1-y_2)) - 2\exp(\lambda_2(1-y_2))], \end{cases} \tag{4}$$

y_1, y_2 is the reduced volume,

$$\begin{cases} y_1 = a/r_{01} = (V/V_{01})^{1/3}, \quad V_{01} = N(r_{01})^3/\gamma, \\ y_2 = a/r_{02} = (V/V_{02})^{1/3}, \quad V_{02} = N(r_{02})^3/\gamma, \end{cases} \tag{5}$$

where r_{01}, r_{02} is the equilibrium distance, ε_1, ε_2 is the corresponding well depth, λ_1, λ_2 describe the decrease in potential as the distance increases. γ is the structural constant, for fcc structure, we have $\gamma = \sqrt{2}$. The volume of the fcc solid is $V = Na^3/\gamma$. Si_3N_4 is not the fcc solid and the different phases have different crystal structure, i.e., the structure constant should take different values for different phases. However, our calculations show that the results are not sensitive to the values of γ, thus we take $\gamma = \sqrt{2}$ for all phases.

The $g(r,V)$ in Eq. (2) is the potential energy of an atom as it roams from the center atom to a distance r. In terms of the AMFP approach [19–22], $g(r,V)$ can be expressed by $E_2(a)$ as follows:

$$g(r,V) = \frac{1}{2}\left[\left(1+\frac{r}{a}\right)E_2(a+r) + \left(1-\frac{r}{a}\right)E_2(a-r) - 2E_2(a)\right]. \tag{6}$$

r_{m} is the largest displacement, its value can be approximately taken as the Wigner–Seitz radius, $r_{\mathrm{m}} = (3a^3/4\pi\gamma)^{1/3} \approx a/2$.

In order to consider the quantum effect, we develop $g(r, V)$ into the quadratic function in the equilibrium position

$$g(r,V) = \frac{1}{2}\mu\omega^2 r^2 = \frac{1}{2}\left[\frac{\partial^2 E_2(a)}{\partial a^2} + \frac{2}{a}\frac{\partial E_2(a)}{\partial a}\right] r^2. \tag{7}$$

In terms of Eq. (7), the harmonic vibration frequency ω and the Einstein temperature Θ_{E} can be determined as

$$\Theta_{\mathrm{E}} = \frac{\hbar\omega}{k} = \frac{\hbar}{k\sqrt{\mu}}\left[\frac{\partial^2 E_2(a)}{\partial a^2} + \frac{2}{a}\frac{\partial E_2(a)}{\partial a}\right]^{1/2}$$

$$= \frac{\hbar}{kr_{02}\sqrt{\mu}}\left[\frac{\partial^2 E_2(a)}{\partial y_2^2} + \frac{2}{y_2}\frac{\partial E_2(a)}{\partial y_2}\right]^{1/2}. \tag{8}$$

The Grüneisen parameter can be derived as

$$\gamma_{\mathrm{G}} = -\frac{V}{\Theta_{\mathrm{E}}}\frac{\partial\Theta_{\mathrm{E}}}{\partial V} = -\frac{y_2}{3\Theta_{\mathrm{E}}}\frac{\partial\Theta_{\mathrm{E}}}{\partial Y_2}$$

$$= -\frac{1}{6}\frac{\partial^3 E_2/\partial y_2^3 + (2/y_2)\partial^2 E_2/\partial y_2^2 - (2/y_2^2)\partial E_2/\partial y_2}{\partial^2 E_2/\partial y_2^2 + (2/y_2)\partial E_2/\partial y_2}. \tag{9}$$

For simplicity, we introduce dimensionless reduced free volume $\bar{\nu}_{\mathrm{f}}$ and reduced radial coordinate x as follows:

$$\nu_{\mathrm{f}} = 4\pi a^3\bar{\nu}_{\mathrm{f}} = 4\pi\gamma V\bar{\nu}_{\mathrm{f}}, \tag{10}$$

$$x = r/a, \qquad x_{\mathrm{m}} = \frac{r_{\mathrm{m}}}{a} \approx \frac{1}{2}. \tag{11}$$

The reduced free volume $\bar{\nu}_{\mathrm{f}}$ and its derivatives with respect to temperature and reduced volume can be expressed as

$$\bar{\nu}_{\mathrm{f}} = \int_0^{x_{\mathrm{m}}} \exp(-g(x,y_2)/kT)x^2\mathrm{d}x, \tag{12}$$

$$\bar{\nu}_{\mathrm{f}a} = T\frac{\partial}{\partial T}\bar{\nu}_{\mathrm{f}} = \frac{1}{kT}\int_0^{x_{\mathrm{m}}} \exp(-g(x,y_2)/kT)g(x,y_2)x^2\mathrm{d}x, \tag{13}$$

$$\bar{\nu}_{\mathrm{f}b} = -\frac{\partial}{\partial y_2}\bar{\nu}_{\mathrm{f}} = \frac{1}{kT}\int_0^{x_{\mathrm{m}}} \exp(-g(x,y_2)/kT)\frac{\partial}{\partial y_2}g(x,y_2)x^2\mathrm{d}x. \tag{14}$$

Here $g(x, y_2) \equiv g(r, V)$, combining Eqs. (4), (6) and (10), we have

$$g(x,y_2) \equiv g(r,V) = \frac{1}{2}[(1+x)E_2(y_2 + y_2x)$$

$$+(1-x)E_2(y_2 - y_2x) - 2E_2(y_2)]. \tag{15}$$

The compressibility factor can be derived as

$$Z = \frac{PV}{NkT} = -\frac{a}{3}\frac{\partial}{\partial a}\frac{F}{NkT} = \frac{P_{\mathrm{c}}V}{NkT} + \frac{P_{\mathrm{f}}V}{NkT} + \frac{P_{\mathrm{qm}}V}{NkT}, \tag{16}$$

where $\frac{P_{\rm c}V}{NkT}$, $\frac{P_{\rm f}V}{NkT}$, and $\frac{P_{\rm qm}V}{NkT}$ represent the contribution of cold energy, the contribution of the free volume, and the quantum modification, respectively.

$$\frac{P_{\rm c}V}{NkT} = -\frac{a}{3kT}\frac{\partial}{\partial a}[E_1(y_1) + E_2(y_2)] = -\frac{y_1}{3kT}E_1'(y_1) - \frac{y_2}{3kT}E_2'(y_2), \tag{17}$$

$$\frac{P_{\rm f}V}{NkT} = 1 + \frac{y_2}{3\bar{\nu}_{\rm f}}\frac{\partial}{\partial y_2}\bar{\nu}_{\rm f} = 1 - \frac{y_2\bar{\nu}_{{\rm f}b}}{3\bar{\nu}_{\rm f}}, \tag{18}$$

$$\frac{P_{\rm qm}V}{NkT} = \frac{\gamma_{\rm G}U_{\rm qm}}{NkT}. \tag{19}$$

The internal energy can be derived as

$$\frac{U}{NkT} = -T\frac{\partial}{\partial T}\frac{F}{NkT} = \frac{3}{2} + \frac{1}{kT}[E_1(y_1) + E_2(y_2)] + \frac{T}{\bar{\nu}_{\rm f}}\frac{\partial\bar{\nu}_{\rm f}}{\partial T}$$

$$= \frac{3}{2} + \frac{1}{kT}[E_1(y_1) + E_2(y_2)] + \frac{\bar{\nu}_{{\rm f}a}}{\bar{\nu}_{\rm f}} + \frac{U_{\rm qm}}{NkT}, \tag{20}$$

where the first term represent the ideal gas, the second term, the third term and the fourth term represent the contribution of cold energy, the contribution of the free volume, and the quantum modification, respectively.

$$\frac{U_{\rm qm}}{NkT} = -T\frac{\partial}{\partial T}\frac{F_{\rm qm}}{NkT} = \frac{3\Theta_{\rm E}/T}{{\rm e}^{\Theta_{\rm E}/T} - 1} - 3. \tag{21}$$

By using the above equations, all other thermodynamic quantities can be analytically derived. The derivations are straightforward. However, the expressions for thermal expansion coefficient, compressibility coefficient and isochoric heat capacity are redundant, we would calculate these quantities by using numerical differentiation instead of the analytic expressions. The compressibility factor can be seen as function of variables T and V, $Z = Z(T, V)$. In terms of the function, the formulae for thermal expansion coefficient, compressibility coefficient, and isochoric heat capacity can be reduced to the following form:

$$\alpha = \frac{1}{V}\left(\frac{\partial V}{\partial T}\right)_P = \left[\frac{Z}{T} + \left(\frac{\partial Z}{\partial T}\right)_V\right]\left[Z - V\left(\frac{\partial Z}{\partial V}\right)_T\right]^{-1}, \tag{22}$$

$$\beta = -\frac{1}{V}\left(\frac{\partial V}{\partial P}\right)_T = \left(\frac{V}{NkT}\right)\left[Z - V\left(\frac{\partial Z}{\partial V}\right)_T\right]^{-1}, \tag{23}$$

$$\frac{C_V}{Nk} = \frac{1}{Nk}\left(\frac{\partial U}{\partial T}\right)_V = \frac{U}{NkT} + T\frac{\partial}{\partial T}\left(\frac{U}{NkT}\right)_V. \tag{24}$$

In our calculations, it is found that the following steps for the numerical differentiations in Eqs. (22)–(24) can reach stable numerical results, $\Delta T = 0.00001 \times T$ and $\Delta V = 0.00001 \times V$.

3. Results and discussion

In this section, we apply the above formalism to α-, β-, and γ-Si_3N_4. We determine the parameters for the Morse potential in Eq. (4) by fitting the compression experimental data of α-, β-, and γ-Si_3N_4 [8, 13, 14]. The determined values

of these parameters are listed in Table. Furthermore, we calculate the numerical results of the pressure dependence of the molar volume at room temperature by using the AMFP, and compare our results with the available experimental data [8, 13, 14] in Figs. 1–3. It is shown that our results are in good agreement with the

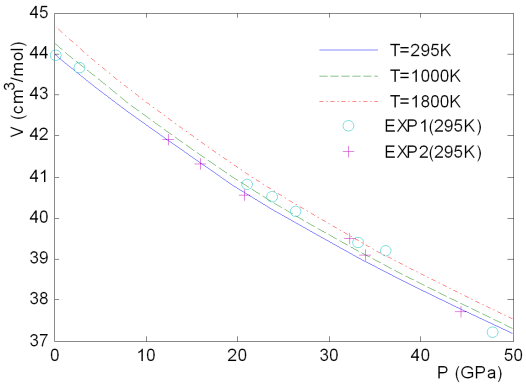

Fig. 1. Comparison of the pressure dependence of the molar volume of α-Si_3N_4 calculated by using the AMFP at 295 K (solid line) with the experimental data by Kruger et al. in Ref. [8] at 295 K. Open circles and cross marks show the compression experimental data and decompression experimental data, respectively. Furthermore, comparison of the pressure dependence of the molar volume calculated at 295 K (solid line) with the results predicted at 1000 K (dashed line), 1800 K (dash-dotted line).

TABLE

Parameter values of the Morse potential for α-, β-, and γ-Si_3N_4: the well depth in K, the equilibrium volume in cm^3 mol^{-1}.

Si_3N_4	ε_1 [K]	λ_1	V_{01} [cm^3/mol]	ε_2 [K]	λ_2	V_{02} [cm^3/mol]
α	110	2.7	155	390000	2.007	43.948
β	65000	2.8	43.69	270000	2.6	43.88
γ	95000	3	34.94	96500	2.865	34.91

available experimental data. This suggests that the AMFP is a useful approach to study the thermodynamic properties of Si_3N_4. At the same time, we predict the pressure dependence of the molar volume at several higher temperatures ($T = 1000$ and 1800 K), and also plot the results in Figs. 1–3. The results suggest that the molar volume of α-, β-, and γ-Si_3N_4 decreases with pressure and increases with temperature.

Substituting the determined parameter values (Table) into Eq. (4), we can obtain the specific form of $E_1(a)$, $E_2(a)$, and $E_c(a)$, for α-, β- and γ-Si_3N_4. We plot

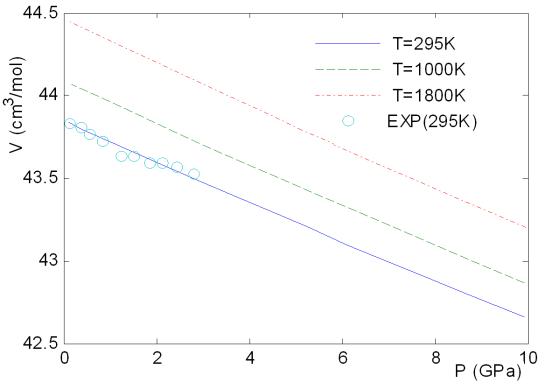

Fig. 2. Comparison of the pressure dependence of the molar volume of β-Si_3N_4 calculated by using the AMFP at 295 K (solid line) with the experimental data by Cartz and Jorgensen in Ref. [13] at 295 K. Open circles represent the compression experimental data. Furthermore, comparison of the pressure dependence of the molar volume calculated at 295 K (solid line) with the results predicted at 1000 K (dashed line), 1800 K (dash-dotted line).

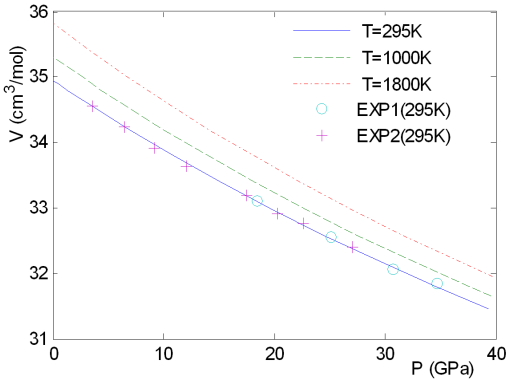

Fig. 3. Comparison of the pressure dependence of the molar volume of γ-Si_3N_4 calculated by using the AMFP at 295 K (solid line) with the experimental data by Soignard et al. in Ref. [14] at 295 K. Open circles and cross marks show the compression experimental data and decompression experimental data, respectively. Furthermore, comparison of the pressure dependence of the molar volume calculated at 295 K (solid line) with the results predicted at 1000 K (dashed line), 1800 K (dash-dotted line).

$E_1(a)$, $E_2(a)$, and $E_c(a)$ versus the nearest-neighbor distance of α-, β-, and γ-Si_3N_4 in Figs. 4–6, respectively. From these figures, we can see that the proportion of $E_1(a)$ in the cohesive energy $E_c(a)$ increases gradually with the sequence of α-Si_3N_4 to β-Si_3N_4 and to γ-Si_3N_4. This suggests that the contribution of $E_1(a)$ to the cohesive energy $E_c(a)$ increases gradually with the sequence of α-Si_3N_4 to β-Si_3N_4 and to γ-Si_3N_4.

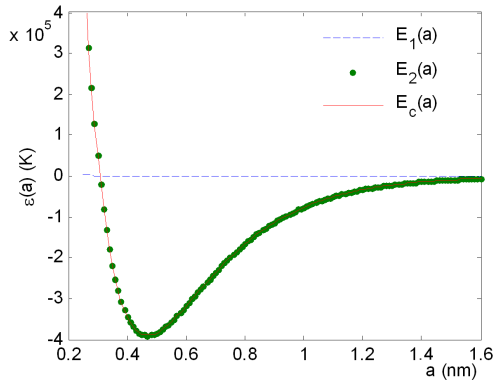

Fig. 4. Potential energy as function of the nearest-neighbor distance calculated for α-Si_3N_4. $E_1(a)$ (dashed line) represents the partial contribution of chemical bond. $E_2(a)$ (dotted) represents the contribution of the van der Waals interaction between atoms. $E_c(a)$ (solid line) represents the cohesive energy of an atom.

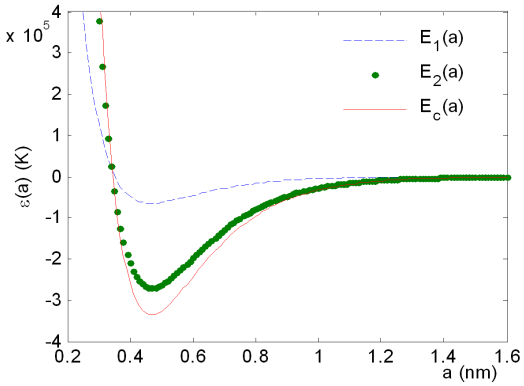

Fig. 5. As for Fig. 4, but for β-Si_3N_4.

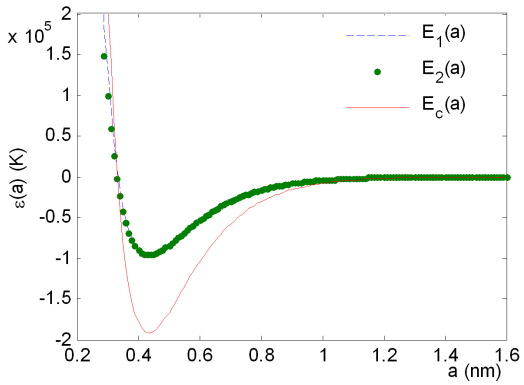

Fig. 6. As for Fig. 4, but for γ-Si_3N_4.

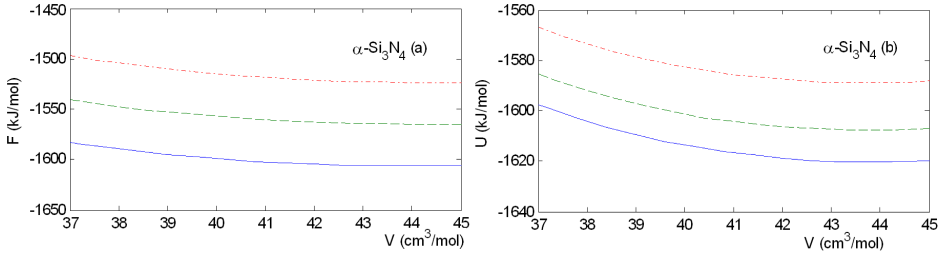

Fig. 7. Free energy (a) and internal energy (b) as functions of the molar volume calculated for α-Si_3N_4 at three temperatures by using the AMFP. The three different lines represent the results for $T = 295$ K (solid line), $T = 1000$ K (dashed line), $T = 1800$ K (dash-dotted line), respectively.

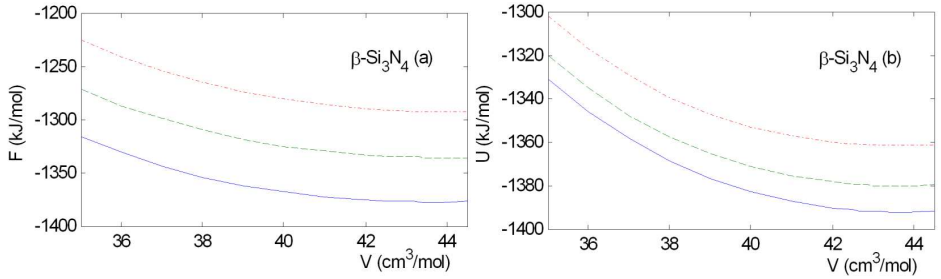

Fig. 8. As for Fig. 7, but for β-Si_3N_4.

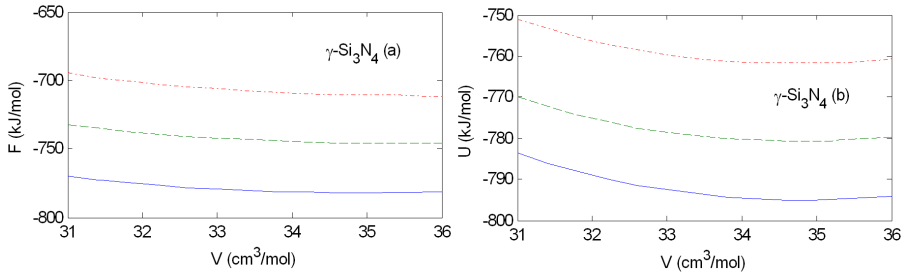

Fig. 9. As for Fig. 7, but for γ-Si_3N_4.

The calculated free energy and internal energy as functions of the molar volume for α-, β-, and γ-Si_3N_4 at various temperatures are shown in Figs. 7–9, respectively. The free energy and internal energy of α-, β-, and γ-Si_3N_4 decrease monotonically with the molar volume. The variation tendency of them with the molar volume is identical at three different temperatures. On the other hand, the free energy and internal energy increase with temperature. Besides, the values of them are negative and very large. This suggests that the interatomic interaction of Si_3N_4 is very strong. It decreases with the molar volume at high pressure and approaches to flat at low pressure.

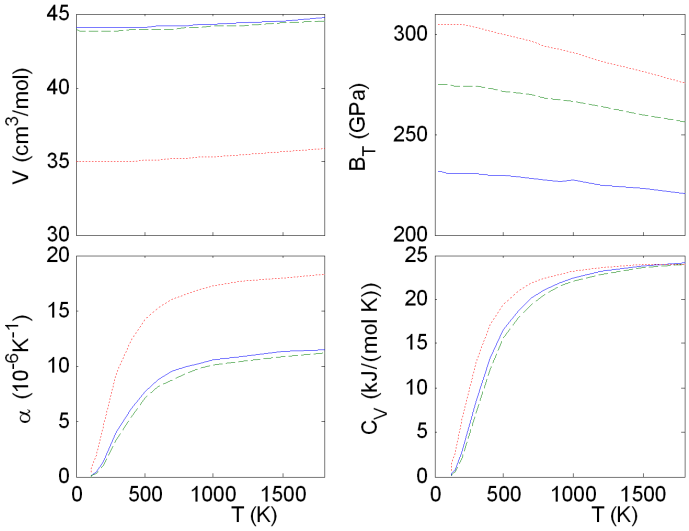

Fig. 10. Temperature dependence of the molar volume, bulk modulus, thermal expansion coefficient and isochoric heat capacity for α-, β-, and γ-Si_3N_4 at zero pressure. The three different lines represent the calculated results for α-Si_3N_4 (solid line), β-Si_3N_4 (dashed line) and γ-Si_3N_4 (dash-dotted), respectively. The molar volume is in $cm^3\ mol^{-1}$, the bulk modulus is in GPa, the thermal expansion coefficient is in $10^{-6}\ K^{-1}$, the isochoric heat capacity is in kJ $mol^{-1}\ K^{-1}$.

The temperature dependence of the molar volume, bulk modulus, thermal expansion coefficient, and isochoric heat capacity for α-, β-, and γ-Si_3N_4 at zero pressure from theoretical calculation in this paper are shown in Fig. 10. The molar volume of Si_3N_4 increases slowly with temperature. The molar volume of γ-Si_3N_4 is the smallest, β-Si_3N_4 is next, α-Si_3N_4 is the largest. This means that the density of γ-Si_3N_4 is the largest, β-Si_3N_4 is next, α-Si_3N_4 is the smallest. On the other hand, the bulk modulus of Si_3N_4 decreases slowly with temperature. The bulk modulus of γ-Si_3N_4 is the largest, β-Si_3N_4 is next, then α-Si_3N_4. The thermal expansion coefficient and isochoric heat capacity increase with temperature. The thermal expansion coefficient and isochoric heat capacity of γ-Si_3N_4 is the largest, α-Si_3N_4 is next, β-Si_3N_4 is the smallest. Additionally, it is worth pointing out that our calculated results of the thermal expansion coefficient are in good agreement with the available experimental data [10–12]. This further verifies that the AMFP is a very useful approach to study the thermodynamic properties of Si_3N_4.

4. Conclusion

In summary, the AMFP approach has been applied to α-, β-, and γ-Si_3N_4. The analytic expressions for the Helmholtz free energy, internal energy and EOS have been derived. By fitting the compression experimental data of α-, β-, and γ-Si_3N_4, we determine the parameters for the Morse potential. Additionally, we

calculate the pressure dependence of the molar volume for α-, β-, and γ-Si_3N_4 at room temperature by using the AMFP. The results obtained are in good agreement with the available experimental data. This suggests that the AMFP is an appropriate approach to study the thermodynamic properties of Si_3N_4. Furthermore, we predict the pressure dependence of the molar volume at several higher temperatures and present the potential function of α-, β-, and γ-Si_3N_4 from theoretical calculation. By means of formalism derived in this paper, we also predict the variation of the free energy and internal energy with the molar volume at several higher temperatures and calculate the temperature dependence of the molar volume, bulk modulus, thermal expansion coefficient and isochoric heat capacity at zero pressure.

Acknowledgments

This work was supported by the Support Programs for Academic Excellence of Sichuan Province of China under grant No. 06ZQ026-010, under grant No. NCET-05-0799 of the Education Ministry of China, and under grant No. 23601008 of UESTC.

References

[1] R. Grün, *Acta Crystallogr., Sect. B: Struct. Crystallogr. Cryst. Chem.* **35**, 800 (1979).

[2] A. Zerr, G. Miehe, G. Serghiou, M. Schwarz, E. Kroke, R. Riedel, H. Fuess, P. Kroll, R. Boehler, *Nature (London)* **400**, 340 (1999).

[3] R.J. Brook, *Nature (London)* **400**, 312 (1999).

[4] I. Tanaka, F. Oba, T. Sekine, E. Ito, A. Kuba, K. Tastumi, H. Adach, T. Yamamoto, *J. Mater. Res.* **17**, 731 (2002).

[5] A. Zerr, M. Kempf, M. Schwarz, E. Kroke, M. Goken, R. Riedel, *J. Am. Ceram. Soc.* **85**, 86 (2002).

[6] J.Z. Jiang, F. Kragh, D.J. Frost, K. Stahl, H. Lindelov, *J. Phys., Condens. Matter* **13**, L515 (2001).

[7] F.L. Riley, *J. Am. Ceram. Soc.* **83**, 245 (2000).

[8] M.B. Kruger, J.H. Nguyen, Y.M. Li, W.A. Caldwell, M.H. Manghnani, R. Jeanloz, *Phys. Rev. B* **55**, 3456 (1997).

[9] J.Z. Jiang, H. Lindelov, L. Gerward, K. Stahl, J.M. Recio, P. Mori-Sanchez, S. Carlson, M. Mezouar, E. Dooryhee, A. Fitch, D.J. Frost, *Phys. Rev. B* **65**, 161202 (2002).

[10] W. Paszkowicz, R. Minikayev, P. Piszora, M. Knapp, C. Bähtz, J.M. Recio, M. Marqués, P. Mori-Sánchez, L. Gerward, J.Z. Jiang, *Phys. Rev. B* **69**, 052103 (2004).

[11] K. Kato, I. Inoue, K. Kijima, I. Kawada, H. Tananka, T. Yamane, *J. Am. Ceram. Soc.* **58**, 90 (1975).

[12] R.J. Bruls, H.T. Hintzen, G. de With, R. Metselaar, J.C. van Miltenburg, *J. Phys. Chem. Solids* **62**, 783 (2001).

[13] L. Cartz, J.D. Jorgensen, *J. Appl. Phys.* **52**, 236 (1981).

[14] E. Soignard, M. Somayazulu, J.J. Dong, O.F. Sankey, P.E. McMillan, *J. Phys., Condens. Matter* **13**, 557 (2001).

[15] W.Y. Ching, L. Ouyang, J.D. Gale, *Phys. Rev. B* **61**, 8696 (2000).

[16] R. Belkada, T. Shibayanagi, M. Naka, *J. Am. Ceram. Soc.* **83**, 2449 (2000).

[17] S. Ogata, N. Hirosaki, C. Kocer, H. Kitagawa, *Phys. Rev. B* **64**, 172102 (2001).

[18] C.M. Fang, G.A. de Wijs, H.T. Hintzen, G.J. de With, *J. Appl. Phys.* **93**, 5175 (2003).

[19] Y. Wang, D. Chen, X. Zhang, *Phys. Rev. Lett.* **84**, 3220 (2000).

[20] Y. Wang, *Phys. Rev. B* **62**, 196 (2000).

[21] Y. Wang, *Phys. Rev. B* **63**, 245108 (2001).

[22] Y. Wang, R. Ahuja, B. Johansson, *Phys. Rev. B* **65**, 014104 (2001).

[23] N.K. Bhatt, A.R. Jani, P.R. Vyas, V.B. Gohel, *Physica B* **65**, 014104 (2001).

[24] N.K. Bhatt, P.R. Vyas, A.R. Jani, V.B. Gohel, *J. Phys. Chem. Solids* **66**, 797 (2005).

[25] J.X. Sun, L.C. Cai, Q. Wu, F.Q. Jing, *Phys. Rev. B* **71**, 024107 (2005).

[26] L.A. Girifalco, *J. Phys. Chem.* **96**, 858 (1992).

[27] J.X. Sun, *Physica B* **34**, 381 (2006).

[28] M.C. Abramo, C. Caccamo, *J. Phys. Chem. Solids* **57**, 1751 (1996).

[29] M.C. Abramo, C. Caccamo, D. Costa, G. Pellicane, R. Ruberto, *Phys. Rev. E* **69**, 031112 (2004).

[30] V.I. Zubov, N.P. Tretiakov, J.F. Sanchez, A.A. Caparica, *Phys. Rev. B* **53**, 12080 (1996).

[31] V.I. Zubov, J.F. Sanchez-Ortiz, N.P. Tretiakov, I.V. Zubov, *Phys. Rev. B* **55**, 6747 (1997).

[32] Z.W. Salsburg, W.W. Wood, *J. Chem. Phys.* **37**, 798 (1962).

[33] F.H. Ree, A.C. Holt, *Phys. Rev. B* **8**, 826 (1973).

[34] K. Westera, E.R. Cowley, *Phys. Rev. B* **11**, 4008 (1975).

[35] E.R. Cowley, J. Gross, Zhaoxin Gong, G.K. Horton, *Phys. Rev. B* **42**, 3135 (1990).

[36] A.C. Holt, M. Ross, *Phys. Rev. B* **1**, 2700 (1970).

[37] E. Wasserman, L. Stixrude, *Phys. Rev. B* **53**, 8296 (1996).

[38] J.X. Sun, H.C. Yang, Q. Wu, L.C. Cai, *J. Phys. Chem. Solids* **63**, 113 (2002).